Nematic Ordering in Mixtures of Polymers and Liquid Crystals

Akihiko Matsuyama*
(Department of Chemistry for Materials)

(Received August 30, 2002)

Abstract

We review our recent theoretical works on the phase ordering in mixtures of polymers and liquid crystals. A mean field theory is introduced to describe nematic-isotropic phase transitions and phase separations in binary mixtures of a low-molecular weight liquid crystal molecule and a polymer chain which has various degrees of flexibility. We calculate the phase diagrams on the temperature-concentration plane, depending on the stiffness of polymer chains and the strength of anisotropic interactions between rigid molecules. We also study spinodal decomposition (SD) in polymer/liquid crystal mixtures by solving linearized time-dependent Landau-Ginzburg equations for concentration (conserved order parameter) and orientation (nonconserved order parameter). We find a new SD process driven by instability of the orientational order parameter. The simulations in two dimension are consistent with the analytical results.

Keywords: polymer dispersed liquid crystals, phase separations, spinodal decompositions, nematic-isotropic phase transitions

1 Introduction

Mesomorphic mixtures comprising of polymers and liquid crystal molecules (so called *polymer dispersed liquid crystals*: PDLC) are of interest because of their important technological applications in high modulus fibers, nonlinear optics, and electro-optical devises. The performances of these systems are closely related to a chain extension in a liquid crystal phase and phase separations[1]. Low-molecular weight liquid crystals are modeled as rigid rodlike molecules. On the other hand, polymer chains have the variety of their stiffness and so when the polymer chains are mixed with the liquid crystal molecules we can expect various types of phase diagrams depending on the stiffness of the polymer chain.

In mixtures of a flexible polymer and a liquid crystal, broad biphasic regions between an isotropic phase and a nematic phase appear below the nematic-isotopic transition (NIT) temperature of the pure liquid crystal molecule. The liquid crystalline phases are destroyed as increasing

*email: matuyama@chem.mie-u.ac.jp

the polymer concentration. These nematic-isotropic phase separations have been investigated both experimentally[2-8] and theoretically[8-14]. In contrast, mixtures of a liquid crystalline polymer and a liquid crystal have good miscibility even at a liquid crystalline phase[15]. In these systems it is important to consider the co-occurrences of orientational ordering of the polymer chain and phase separations[16-19].

In this review we introduce a mean field theory to describe phase behaviors in binary mixtures of a liquid crystal molecule and a polymer chain which has various degrees of flexibility. We calculate the phase diagrams on the temperature-concentration plane. We also study the phase separation dynamics (spinodal decompositions) by solving linearized time-dependent Landau-Ginzburg equations for concentration (conserved order parameter) and orientation (nonconserved order parameter) and show simulations in two dimensions.

2 Free Energy for Mixtures of a Polymer and a Liquid Crystal

Consider binary mixtures of a non-nematic polymer and a liquid crystal (nematogen). The polymers and liquid crystals interact through orientational dependent van der waals interactions and excluded volume interactions. We here assume that the two neighboring bonds on the polymer chains have either bent or straightened conformations[20, 21] and the conformational energy of the straightened bond is $|\epsilon_0|$ less than that of the bent bonds. The straightened state of the bonds on the chains is energetically favored and, however, it is entropically unfavorable. The nematic behaviors of the straightened bonds as well as liquid crystals can be induced by the anisotropic interactions. To describe the nematic-isotropic phase transition and phase separations, we consider thermodynamics of our systems. Hereafter we refer the segments in straightened bonds as "rigid" segments.

Let N_p and N_ℓ be the number of the polymers and the liquid crystal molecules, respectively. Let n_p be the number of segments on the polymer and n_ℓ be that of the liquid crystal. The total lattice sites of our systems is given by $N_t = n_\ell N_\ell + n_p N_p$ and $\phi = n_p N_p / N_t$ is the volume fraction of the polymer chains. The volume fraction of the liquid crystals is given by $\phi_\ell = 1 - \phi$. The free energy of our systems can be given by

$$F = F_{bent} + F_{mix} + F_{nem}. \tag{1}$$

The first term shows the free energy change needed to straighten bent bonds on the polymers and is given by[21, 22]

$$\beta F_{bent} = N_p \Big[n_r(\beta f_0) - S_{comb}/k_B - \Delta S_{conf}/k_B \Big], \tag{2}$$

where $\beta \equiv 1/k_B T$, T is the absolute temperature, k_B is the Boltzmann constant, f_0 is the local free energy difference between the bent and straightened conformations, and n_r shows the number of the rigid segments on the polymer chain. We here assume that each chain has the same conformation. The second term in Eq. (2) is the combinatorial entropy related to the number of ways to select n_r rigid segments out of the n_p segments on the polymer and is given $S_{comb}/k_B = -n_p[x \ln x + (1-x)\ln(1-x)]$, where $x(\equiv n_r/n_p)$ shows the fraction of the rigid segments on the polymer chain. The volume fraction ϕ_r of the rigid (straightened) segments on the polymer chain is given by $\phi_r = n_r N_p / N_t = x\phi$. The third term in Eq. (2) shows the change in conformational entropy to bring a chain from a crystalline (straightened) state to a flexible

amorphous state. According to the Flory's lattice theory, the conformational entropy $S_{conf}(n)$ of the polymer chain with n flexible segments is given by *entropy of disorientation*[23]. When the n_r segments out of the n_p segments on a polymer chain are replaced by rigid segments, the conformational entropy change ΔS_{conf} is given by $\Delta S_{conf} = S_{conf}(n_p - n_r) - S_{conf}(n_p)$.

The second term in Eq. (1) is the free energy of the isotropic mixing for the polymers and liquid crystals. According to the Flory theory, the free energy is given by[23]

$$\beta F_{mix}/N_t = \frac{1-\phi}{n_\ell}\ln(1-\phi) + \frac{\phi}{n_p}\ln\phi + \chi\phi(1-\phi), \tag{3}$$

where $\chi(\equiv U_0/k_BT)$ is the Flory-Huggins interaction parameter related to the isotropic van der waals interactions between unlike molecular species.[23]

The third term in Eq. (1) shows the free energy for the nematic ordering. On the basis of both the Maier-Saupe model[24, 25] for orientational dependent-attractive interactions and the Onsager model[26] for excluded volume interactions, the free energy of the nematic ordering is given by

$$\begin{aligned}\beta F_{nem}/N_t &= \frac{1-\phi}{n_\ell}\int f_\ell(\theta)\ln 4\pi f_\ell(\theta)d\Omega + \frac{\phi_r}{n_r}\int f_r(\theta)\ln 4\pi f_r(\theta)d\Omega - \frac{1}{2}\nu_{\ell\ell}S_\ell^2(1-\phi)^2 \\ &\quad -\nu_{\ell r}S_\ell S_r(1-\phi)\phi_r + (\rho_{\ell\ell}-1)(1-\phi)^2 + 2(\rho_{\ell r}-1)(1-\phi)\phi_r,\end{aligned} \tag{4}$$

where $d\Omega \equiv 2\pi\sin\theta d\theta$, θ is the angle between the rigid segments and the director of the orienting field. The $\nu_{\ell\ell}$ shows the orientational dependent (Maier-Saupe) interactions between the liquid crystals, $\nu_{\ell r}$ is that between the liquid crystal and the rigid segment on the polymer chains. We here focus on the nonnematic polymer and so we can neglect the terms of the anisotropic interaction ν_{rr} and the excluded volume interaction ρ_{rr} between rigid segments on the polymer chain in Eq. (4). The $f_\ell(\theta)$ and $f_r(\theta)$ show the orientational distribution functions of the liquid crystals and that of the rigid segments on the polymers, respectively. The scalar orientational order parameter S_ℓ of the liquid crystals and that S_r of the rigid segments on the polymer is given by

$$S_i = \int P_2(\cos\theta)f_i(\theta)d\Omega, \tag{5}$$

$i = \ell, r$. where $P_2(\cos\theta) \equiv 3(\cos^2\theta - 1/3)/2$. The last two terms in Eq. (4) show the excluded volume interactions and the function ρ_{ij} $(i, j = \ell, r)$ is given by $\rho_{ij} = \frac{4}{\pi}\iint \sin\gamma(\theta,\theta')f_i(\theta)f_j(\theta')d\Omega d\Omega'$. In the isotropic phase, we have $f_i(\theta) = 1/(4\pi)$ and $\rho_{ij} = 1$[26].

The orientational distribution function $f_\ell(\theta)$ of the liquid crystals and $f_r(\theta)$ of the rigid segments on the polymer are determined by the free energy (4) with respect to these functions: $(\partial F_{nem}/\partial f_i(\theta))_{x,f_j} = 0$, under the normalization conditions $\int f_i(\theta)d\Omega = 1$. In the framework of our mean field approximations[21], we obtain the distribution function:

$$f_i(\theta) = \frac{1}{Z_i}\exp[\eta_i P_2(\cos\theta)], \tag{6}$$

$$\eta_\ell \equiv n_\ell\Big[(\nu_{\ell\ell} + \frac{5}{4})S_\ell(1-\phi) + (\nu_{\ell r} + \frac{5}{4})S_r x\phi\Big], \tag{7}$$

$$\eta_r \equiv n_p x(\nu_{\ell r} + \frac{5}{4})S_\ell(1-\phi), \tag{8}$$

where the constants Z_i $(i = \ell, r)$ are determined by the normalization condition as $Z_i = 2\pi I_0[\eta_i]$, where the function $I_0[\eta_i]$ is defined as

$$I_m[\eta_i] \equiv \int_0^1 \Big[P_2(\cos\theta)\Big]^m \exp\Big[\eta_i P_2(\cos\theta)\Big]d(\cos\theta), \tag{9}$$

$m = 0, 1, 2, \cdots$. Substituting Eq. (6) into (5), we obtain two self-consistency equations for the two order parameters S_ℓ and S_r:

$$S_i = I_1[\eta_i]/I_0[\eta_i], \tag{10}$$

and the average value of the order parameters is given by $S = S_\ell(1-\phi) + S_r\phi_r$.

The fraction x of the rigid segments on the polymer chain is determined by minimizing the free energy (1) with respect to x: $(\partial F/\partial x)_{S_\ell,S_r} = 0$. This yields

$$S_r = D(x)/[(\nu_{\ell r} + \frac{5}{4})S_\ell(1-\phi)], \tag{11}$$

$$D(x) \equiv \left[\ln\left[\frac{x}{(1-x)\lambda}\right] + \frac{1}{n_p(1-x)}\right], \tag{12}$$

and $\lambda \equiv (e/(z-1))\exp(-\beta f_0)$, where z is the coordination number of a quasilattice[21]. By solving the coupled equations (10) and (11), we can obtain the values of the two order parameters S_ℓ, S_r, and the fraction x of the rigid segments on the polymer chain as a function of temperature and concentration.

In our numerical calculations, we further split the local free energy difference f_0 in Eq. (2) into two parts: $f_0 = \epsilon_0 - Ts_0$, where $s_0(= k_B \ln\omega_0)$ is the local entropy loss which is given by $\omega_0 = 1/(z-2)$ [20] and $\epsilon_0(< 0)$ is the energy change needed to straighten a bent bond. Then we obtain $\lambda = \omega\exp(-\beta\epsilon_0)$, where $\omega \equiv e/[(z-1)(z-2)]$. The stiffness of the polymer is controlled by the ϵ_0. The larger values of ϵ_0 correspond to the stiffer polymers. The most flexible polymer chain is realized when $\epsilon_0 = 0$. The coexistence curve (binodal) and the spinodal line of the phase diagram can be calculated by the chemical potentials[21]. The anisotropic interaction parameter $\nu_{\ell\ell}$ between liquid crystals is given to be inversely proportional to temperature: $\nu_{\ell\ell} = U_a/k_BT$[25]. We also define the dimensionless nematic interaction parameter $\alpha \equiv \nu_{\ell\ell}/\chi = U_a/U_0$, the stiffness parameter $\epsilon \equiv |\epsilon_0|/U_a$ of a polymer chain and $c \equiv \nu_{\ell r}/\nu_{\ell\ell}$.

3 Phase Diagrams

3.1 Mixtures of a flexible polymer and a liquid crystals

When the polymer chain is sufficiently flexible, we can assume that $S_r = 0$, $\epsilon = 0$, and $\nu_{\ell r} = 0$. The theory results in that for mixtures of a flexible polymer and a liquid crystals[14].

Figure 1(a) shows the binodal curve for $\alpha = 2.5$, $n_r = 2$.The temperature is normalized by the NIT temperature T^L_{NI} of the pure nematogen. The number n_p of segments on a polymer chain is changed. For low molecular weight polymers, the biphasic region between the nematic and isotropic phases (N+I) appears at lower temperatures. The stable nematic phase appears in a dilute region of the polymer concentration. The nematic phase consists almost of pure nematogens and the coexisting isotropic phase consists of nematogens and flexible polymers. For larger values of n_p, we have the isotopic-isotropic (I+I) phase separation with an upper critical solution temperature (UCST) such as observed for polystylene with 7CB[5]. We also find the three phase equilibrium (triple point: TP) where two isotropic phases and a nematic phase can simultaneously coexist. At high temperatures, the system is in isotropic phase (I) because the entropy of mixing is dominant. As decreasing temperature, the I+I phase separation takes place where χ parameter becomes dominant. Further decreasing temperature, the attractive interaction $\nu_{\ell\ell}$ between nematogens dominates and the N+I phase separation occurs at the lower temperature side of the TP.

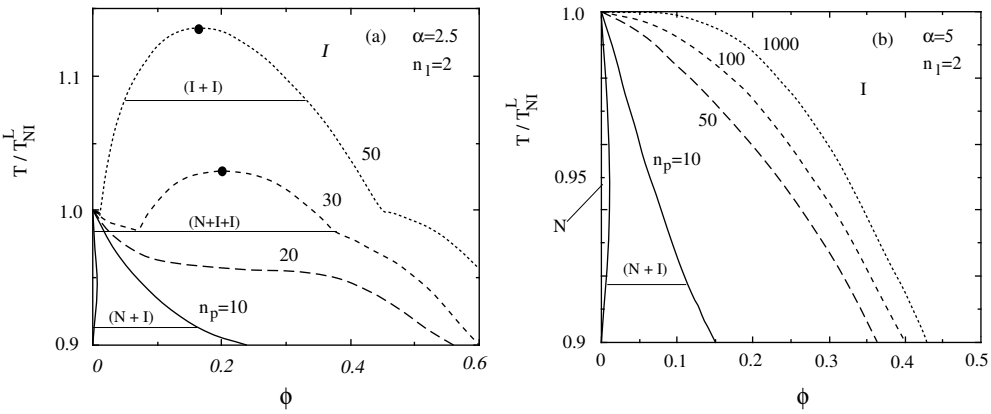

Fig. 1: (a) The binodal curves for $\alpha = 2.5$, $n_r = 2$. The temperature is normalized by the NIT temperature T_{NI}^L of a pure liquid crystal. The number n_p of segments on a polymer chain is changed. (b) The binodal curves for $\alpha = 5$, $n_r = 2$. When the nematic interaction parameter α is increased, the isotropic-isotropic phase separation disappears and we have the nematic-isotropic phase separation

Figure 1(b) shows the phase diagram for $\alpha = 5$ and $n_r = 2$. The number n_p of segments on a polymer is changed. When the nematic interaction parameter α is increased, the isotropic-isotropic phase separation disappears and we only have the nematic-isotropic phase separation. The width of the two phase region increases with increasing n_p. The type of phase diagram is characterized by the nematic interaction parameter α[14, 27].

3.2 Induced-nematic phase

In the following calculations we use $\alpha = 5$, $\epsilon = 3$, $\omega = 0.025$ and $c = 1$ for a typical example[21]. Figure 2 shows the phase diagram on the temperature-concentration plane for $n_\ell = 2$. The number n_p of segments on the polymer is changed from (a) to (b): (a) $n_p = 10$; (b) $n_p = 50$. The temperature is normalized by the NIT temperature T_{NI}^L of the pure liquid crystal molecule. The solid curve is referred to the binodal and the dashed and dotted line shows the spinodal. The short-dashed lines show the NIT line. In the phase diagram, we have two different metastable regions: an isotropic metastable (Im); a nematic metastable (Nm). We also have a nematic unstable region (Nu). As shown in Fig. 2 (a), at higher temperatures we have the two-phase coexistence (N1+I) region between the nematic and the isotropic phase, which was observed in the mixtures of polystyrene (PS) with (p-ethoxybenzylidene)-p-n-butylaniline (EBBA)[2, 3]. The nematic phase (N1) almost consists of the pure liquid crystals and is stabilized by orientational ordering of the liquid crystals. As decreasing temperature, we find a triple point (three phase equilibrium) where the two nematic phases and an isotropic phase can simultaneously coexist (N1+N2+I). At the lower temperature side of the triple point, a new stable nematic phase (N2) is induced by the anisotropic coupling between polymers and liquid crystals. This induced nematic phase (N2) is stabilized by the orientational ordering of both polymer chains and liquid crystals. We also find the (N1+N2) and (N2+I) coexistence regions. As increasing the polymer length n_p,

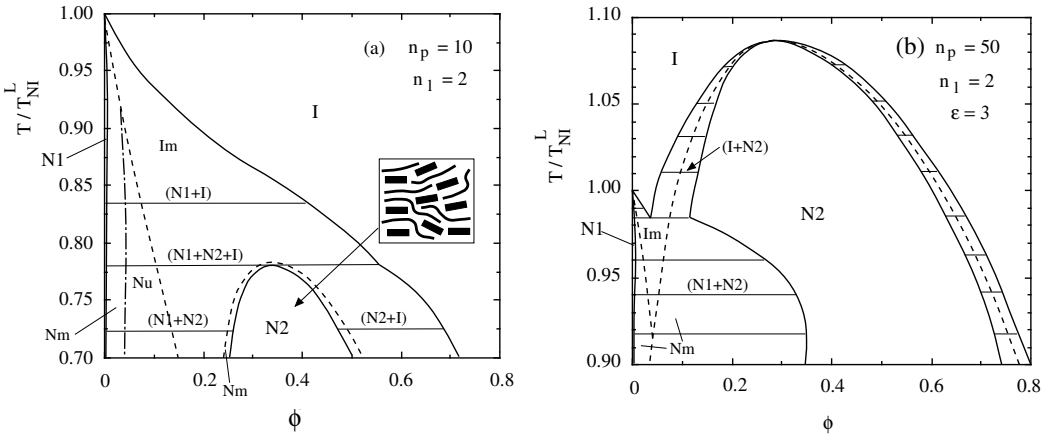

Fig. 2: Phase diagram on the temperature-concentration plane for $n_\ell = 2$. The number n_p of segments on the polymer is changed from (a) to (b): (a) $n_p = 10$; (b) $n_p = 50$.

the induced nematic phase (N2) shifts to higher temperatures due to the correlation between the two neighboring bonds along the polymer chain. In Fig. 2(b), we also find the azeotrope point at which two equilibrium nematic and isotropic phases have the same composition. We predict that the partial orientational ordering of polymers by liquid crystal solvents can give rise to a new stable nematic phase (*induced-nematic phase*), depending on the polymer length and the stiffness of the polymer chain.

4 Phase Separation Dynamics

In this section, we study spinodal decompositions in mixtures of a flexible polymer and liquid crystals. In these mixtures, as shown in Fig.1, biphasic regions between an isotropic and a nematic phase appear below the NIT temperature of the pure liquid crystal molecule. When the system is thermally quenched from a stable isotropic phase into an unstable part of the biphasic region, the fluctuations of concentration and of orientation take place and isotropic or nematic droplets appear with time[28-30]. The instability of these systems is driven by the competition between phase separation and nematic ordering.

To elucidate the time evolution of the concentration and orientation fluctuations during the spinodal decomposition, we calculate structure factor for concentration and for orientation using time-dependent Landau-Ginzburg (TDLG) equations for concentration and orientational order parameters[31]. We also show simulations in two dimension (but without linearization) to further understand our analytical results for the structure factors.

4.1 Kinetic equations

We consider mixtures of a flexible polymer and liquid crystal (nematogen) described by one conserved order parameter (volume fraction ϕ of nematogen) and one nonconserved order pa-

rameter (orientational order parameter S_{ij} of nematogens)[31-36]. Since the orientational order parameter is a traceless symmetric tensor, its components can be expressed as[25]

$$S_{ij} = \frac{d}{2}S(r)\left[n_i(r)n_j(r) - \frac{1}{d}\delta_{ij}\right], \tag{13}$$

where $i, j = x, y, z$ denote the components along three orthogonal coordinate axes, d is the space dimension, $n(r)$ is a local director, δ_{ij} is the Kronecker δ function, and $S(r)$ is the scalar orientational order parameter referred to previously. The dynamics of the mixture is described by the coupled time-dependent Ginzburg-Landau equations[33-36] for the two order parameters. In the inhomogeneous system under nonequilibrium conditions, spatial variations occur in the two order parameters. The total free energy (F) can be expressed in terms of a local bulk free energy density $f(\phi, S_{ij})$ and the gradients of the two order parameters[31]:

$$\begin{aligned} F[\phi, S_{ij}] &= \int dr\Big[f(\phi, S_{ij}) + \frac{K_0}{2}(\nabla\phi)^2 + L_0(\partial_i\phi)(\partial_j S_{ij}) \\ &\quad + \frac{L_1}{2}(\partial_k S_{ij})^2 + \frac{L_2}{2}(\partial_i S_{ik})(\partial_j S_{jk})\Big], \end{aligned} \tag{14}$$

where the free energy F and f are dimensionless quantities (divided by k_BT), T is the absolute temperature, k_B is the Boltzmann constant and K_0, L_0, L_1, L_2 are phenomenological coefficients derived from a mean field theory[33, 34]. In this paper we take these coefficients as constant. The bulk free energy density is given by[31]

$$\begin{aligned} f(\phi, S_{ij}) &= \frac{1-\phi}{n_p}\ln(1-\phi) + \frac{\phi}{n_l}\ln\phi + \chi\phi(1-\phi) \\ &\quad + \frac{1}{2}A(\phi)S_{ij}S_{ji} - \frac{1}{3}B(\phi)S_{ij}S_{jk}S_{ki} + \frac{1}{4}C(\phi)S_{ij}S_{jk}S_{kl}S_{li}, \end{aligned} \tag{15}$$

where the coefficients $A(\phi)$, $B(\phi)$, and $C(\phi)$ are given as a function of temparature and concentration[31].

In considering the nonequilibrium equations of motion for our system, we adopt a thermodynamic point of view. The phenomenological equation of motion for the concentration ϕ, which ensures local conservation of material, is given by[37]:

$$\begin{aligned} \frac{\partial\phi(r,t)}{\partial t} &= \Gamma_\phi\nabla^2\Big(\frac{\delta F}{\delta\phi}\Big) \\ &= \Gamma_\phi\nabla^2\left[\frac{\partial f}{\partial\phi} - K_0\nabla^2\phi - L_0\partial_i\partial_j S_{ij}\right], \end{aligned} \tag{16}$$

where the thermodynamic force which drives the flux is given by the gradient of the chemical potential $\mu = \delta F/\delta\phi$ and Γ_ϕ is the mobility, assumed constant. On the other hand, for the nonconserved order parameter S_{ij}, we take the local rate of change to be linearly proportional to the local thermodynamic force $\partial F/\partial S_{ij}$[37]. The equation of motion for S_{ij} is then given by

$$\begin{aligned} \frac{\partial S_{ij}(r,t)}{\partial t} &= -\Gamma_S\Big(\frac{\delta F}{\delta S_{ij}} + \Lambda(r,t)\delta_{ij}\Big) \\ &= -\Gamma_S\left[\frac{\partial f}{\partial S_{ij}} - L_0\partial_i\partial_j\phi - L_1\nabla^2 S_{ij}\right. \\ &\quad \left. - \frac{L_2}{2}(\partial_i\partial_k S_{kj} + \partial_j\partial_k S_{ki}) + \Lambda(r,t)\delta_{ij}\right], \end{aligned} \tag{17}$$

where the transport coefficients Γ_ϕ and Γ_S are taken as constant. The kinetic equations could in principle be made more general, by writing the Onsager coefficient Γ as a matrix. This would allow one order parameter to be driven by gradients in the chemical potential of the other[33]. However, as this is not the phenomenon under investigation, we set the off-diagonal matrix elements to zero for simplicity. The orientational order parameter evolves in such a way as to lower the free energy, but it must do so subject to the constraint that it remains traceless. The Lagrange multiplier Λ in Eq.(17) will be chosen to ensure conservation of the trace of S_{ij}.

By linearizing Eqs. (16) and (17)[31], we can calculate the structure factor for concentration:

$$S_\phi(q,t) \equiv \langle |\delta\phi(q,t)|^2 \rangle, \tag{18}$$

and that for the component S_{zz} of the orientational order parameter: given by

$$S_S(q,t) \equiv \langle |\delta S_{zz}(q,t)|^2 \rangle, \tag{19}$$

where q is the wave number in the Fourier space and we define a z axis parallel to the director.

4.2 Spinodal decompositions

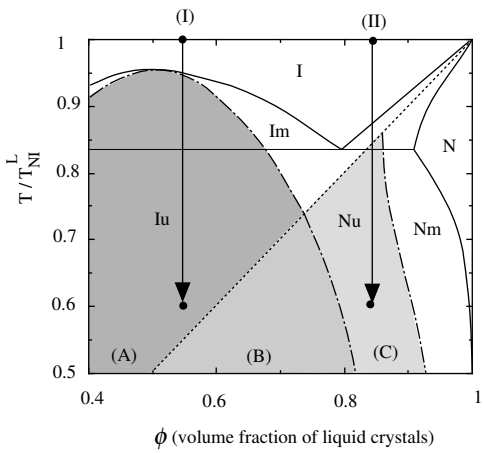

Fig. 3: Phase diagram of a polymer/liquid crystal mixture with $n_p = n_l = 2$ and $\nu/\chi = 1.4$. The solid curve refers to the binodal and the dotted line shows the first-order NIT line. The dash-dotted line shows the spinodal. Closed circles indicate temperature quenches from the stable isotropic phase into the isotropic unstable (Iu; A) and nematic unstable (Nu;B, C) regions.

A typical phase diagram on the temperature-concentration plane is shown in Fig. 3 which is calculated with $n_p = n_l = 2$ and $\nu/\chi = 1.4$ in Eq. (15)[14]. The reduced temperature $\tau(\equiv T/T^L_{NI})$ is normalized by the nematic-isotropic transition (NIT) temperature T^L_{NI} of the pure liquid crystal (at $\phi = 1$). The critical solution point in the isotropic phase is at $\phi = 0.5$ and $\tau = 0.95$. The solid curve refers to the binodal and the dotted line shows the first-order NIT of a hypothetical homogeneous phase. The dash-dotted line shows the spinodal. Note that the origin is suppressed on the ϕ-axis. When $\tau = 0.831$, we have a triple point where two isotropic liquid phases $(L_1 + L_2)$

and a nematic phase (N) can simultaneously coexist. Below the triple point, we have the two-phase coexistence between an isotropic and a nematic phase. Such phase diagrams are observed in mixtures of n-tetracosane and nematic liquid crystal (PAA)[4]. In the biphasic region between the nematic and the isotropic phases, we have two different metastable regions: an isotropic metastable (Im) and a nematic metastable (Nm), and two unstable regions: an isotropic unstable (Iu; A) and a nematic unstable (Nu; B,C)[8, 13, 14]. On increasing the molecular weight n_p of the polymer, the critical solution point shifts to higher temperatures and higher concentrations of mesogens and the Nu and Iu regions also shift to higher temperatures and higher concentrations with increasing n_p[8, 13, 14].

Filled circles indicate temperature quenches from the stable isotropic phase into the isotropic unstable (Iu;A) and nematic unstable (Nu;B, C) regions. The region (A), lying below the isotropic spinodal curve and above the NIT line, corresponds to a system which is initially unstable with respect to concentration fluctuations, but metastable to orientation fluctuations. The region (B), between the isotropic spinodal curve and the NIT line, is initially unstable to both concentration and orientation fluctuations. In the region (C) between the isotropic spinodal curve and the nematic spinodal curve, the system is initially unstable with respect to orientation fluctuations, but metastable to concentration fluctuations. Thus if we thermally quench from an isotropic phase to these different regions, we can expect a variety of SD processes even in the early stages.

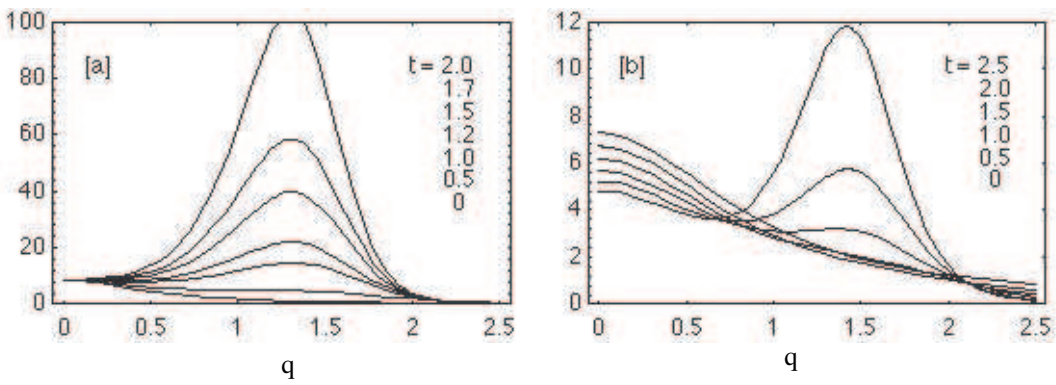

Fig. 4: Temporal evolution of the compositional structure factor (a) S_ϕ and of the orientational structure factor (b) S_S, for the temperature quench into the Iu region A ($\tau = 0.6$, $\phi = 0.55$) in Fig. 3

Figure 4 shows the temporal evolution of the compositional structure factor S_ϕ and of the orientational structure factor S_S, respectively, for the temperature quench into the Iu region ($\tau = 0.6$, $\phi = 0.55$) in Fig. 3. The structure factor for concentration has a maximum at q_m which corresponds to the peak wave number of the growth rate[31]. With time the corresponding mode grows exponentially and the peak position q_m is invariant. The time evolution of the structure factor S_ϕ is the same as that of the Cahn theory for isotropic SD[38, 37]. The structure factor S_S decreases with increasing q at very early times. The amplitude of the peak at $q = 0$ decreases with time because $f_{SS} \equiv (\partial^2 f/\partial S^2) > 0$. With time another peak appears in the S_S curve, corresponding to the peak at q_m, and the orientation fluctuation grows exponentially. In this quench, the concentration fluctuation initially induces the SD and the orientational ordering within the domains subsequently takes place due to the coupling between the two order parameters

as time progresses. Further increasing the initial concentration of mesogen, the orientational

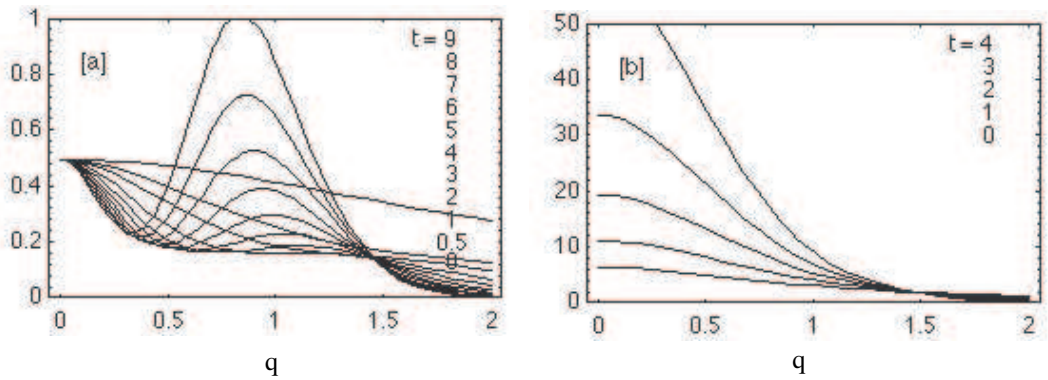

Fig. 5: Temporal evolution of the compositional structure factor (a) S_ϕ and of the orientational structure factor (b) S_S, for the temperature quench into the Nu region C ($\tau = 0.6$, $\phi = 0.85$) in Fig. 3

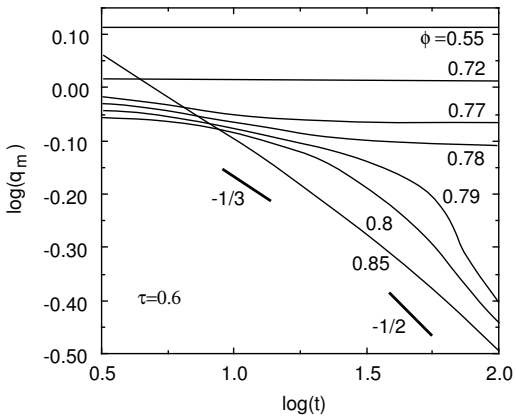

Fig. 6: Temporal evolutions of the scattering wave number q_m at which the compositional structure factor has a maximum. The initial concentration is varied at fixed τ.

fluctuation becomes dominant. Figure 5 shows the temporal evolutions of the structure factors for a temperature quench into the Nu region (C) ($\tau = 0.6$, $\phi = 0.85$), where the system is initially unstable with respect to orientational order parameter ($f_{SS} < 0$) and metastable with respect to concentration ($f_{\phi\phi} \equiv (\partial^2 f/\partial\phi^2) > 0$). In the very early stages, the concentration fluctuation becomes weak with time because $f_{\phi\phi} > 0$. However the orientational fluctuations grow exponentially with time because $f_{SS} < 0$. Further increasing time, a peak in S_ϕ appears and shifts to lower values of the wave number. There is no longer any time stage in which the peak position in S_ϕ is invariant, which was predicted by Cahn's linearized theory for isotropic SD in the early stages[37, 38]. The instability of the orientational ordering initially induces the SD and the concentration fluctuation is induced by the coupling between the two order parameters.

To summarize these results of our linearized analysis, we show in Fig. 6 the values of q_m for the density structure factor S_ϕ for various initial concentrations ϕ_0. In the Iu region A, the peak wave number q_m is invariant during the early stages of the SD. On increasing the initial concentration, we find that the scattering peak shifts to the lower values with time. When $\phi_0 = 0.85$ (region C), the scattering peak for S_ϕ changes as $t^{-1/3}$ (the average domain size increases as $t^{1/3}$ even in the early stages). The instability of the orientational ordering induces the concentration fluctuation through the coupling between two order parameters.

4.3 Simulations in two dimensions

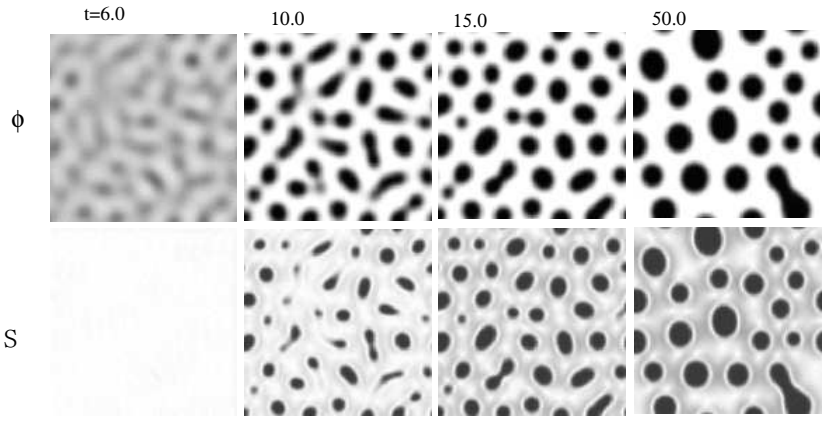

Fig. 7: Time evolution of the compositional (upper) and orientational (lower) order parameters for the temperature quench ($\tau = 0.6$, $\phi_0 = 0.35$) in Fig. 3.

To further understand our analytical results, nonlinear coupled differential equations (16,17) were simulated in two spatial dimensions (x, y) with periodic boundary conditions. In the two dimensions, we have, with the constraints Tr $S_{ii} = 0$ and $S_{ij} = S_{ji}$, a set of two coupled nonlinear partial derivative equations describing the spatiotemporal evolutions of the tensor components S_{xx} and S_{xy} in Eq. (17) and the scalar orientational order parameter is given by $S = 2\sqrt{S_{xx}^2 + S_{xy}^2}$. The time step and grid spacing are $\Delta t = 0.0001$ and $\Delta h = 0.3$ respectively and 128 grid points were used. The initial conditions for the concentration $\phi(x, y)$ and the tensor order parameters $S_{ij}(x, y)$ at each lattice point are given by random numbers distributed uniformly in $\phi(x, y) = \phi_0 \pm 0.02$ and $S_{ij}(x, y) = \pm 0.02$, respectively. Initially, the system is in an isotropic phase. We neglect the random noise terms in the kinetic equations and believe no significant effects on the phase separation dynamics. Figures 7, 8, and 9 show the results of simulations for temperature quenches from the isotropic state to $\tau = 0.6$ with $\phi_0 = 0.35$, $\phi_0 = 0.55$, and $\phi_0 = 0.85$, respectively. The upper(lower) figures show the temporal evolution of the concentration (scalar orientation order parameter). The darkness is proportional to the value of ϕ and S. In region A, at $\phi_0 = 0.33$ [Fig. 7] and $\phi_0 = 0.55$ [Fig. 8] , we first observe the concentration fluctuation in the early stage and the nematogen-rich isotropic droplets appear in a polymer-rich matrix. With time the concentration fluctuation and the orientational fluctuation within the droplets grow and form nematic droplets [Fig. 7] or bicontinuous networks of interconnected domains[Fig. 8].

In the case of $\phi_0 = 0.85$ [region C, Fig. 9], we first observe the orientation fluctuations in

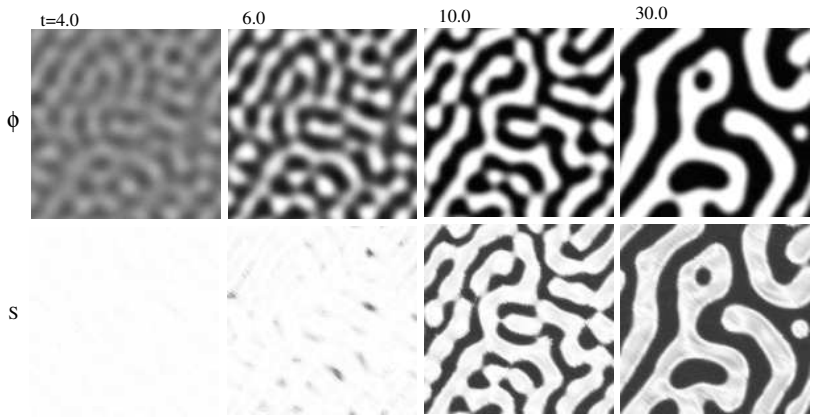

Fig. 8: Time evolution of the compositional (upper) and orientational (lower) order parameters for the temperature quench ($\tau = 0.6$, $\phi_0 = 0.55$) in Fig. 3.

the very early stage ($t = 0.2$), but the system is still in an isotropic state. As time increases, the orientation fluctuations become large and induce concentration fluctuations. We find the polymer-rich isotropic region (white areas) form a fibrillar network morphology in a nematogen-rich nematic matrix ($t \sim 1.0$). Further increasing time, these networks break up ($t = 1.4$) and form polymer-rich isotropic droplets ($t = 12.4$). At late stages ($t = 12.4$), the droplets becomes noncircular in the surrounding nematogen-rich nematic phase. The nematic ordering can significantly influence domain morphology. These simulations show how the phase separation dynamics in polymer/liquid crystal mixtures is driven by the competition between phase separation and nematic ordering. On increasing the concentration of liquid crystal, the instability of the orientational ordering becomes dominant and the mechanism (or morphology) of the SD is changed from concentration fluctuation-induced SD to orientation fluctuation-induced SD. The cross term between gradients plays a significant role in the early stage SD.

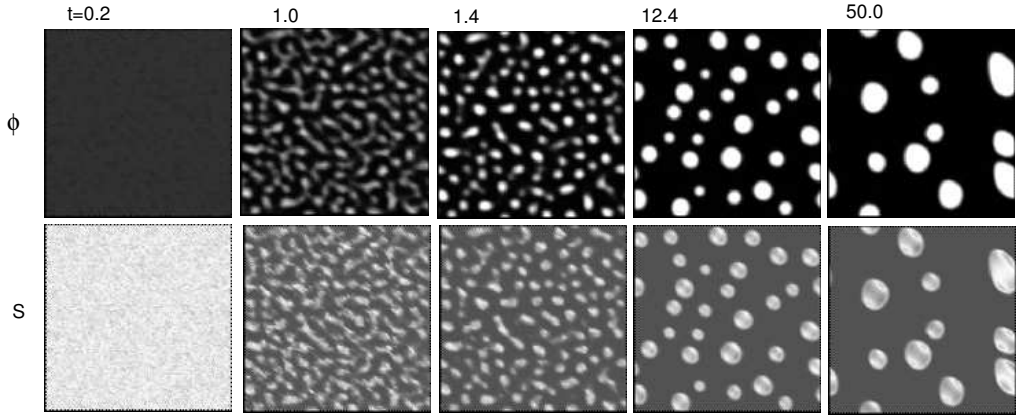

Fig. 9: Time evolution of the compositional (upper) and orientational (lower) order parameters for the temperature quench ($\tau = 0.6$, $\phi_0 = 0.85$) in Fig. 3.

5 Summary

In this review, we have theoretically studied the phase behaviors and phase separation dynamics in mixtures of polymers and liquid crystals. The theory can qualitatively describe the observed phase diagrams. We predict that the partial orientational ordering of polymers by liquid crystal solvents can give rise to a new stable nematic phase (induced nematic phase), depending on the polymer length and the stiffness of the polymer chain. These phase behaviors will be useful for further studies for the polymer dispersed liquid crystals and the investigations of intermolecular interactions, association phenomena, and dipole-dipole correlations between polymers and liquid crystals. Though we have performed a linear analysis of the spinodal decompositions in polymer/liquid crystal mixtures, these results will also be an useful to understand other nematic systems including semiflexible polymer, liquid crystalline polymers, and rodlike colloids[39-42]. The nematic ordering can significantly influence domain morphology.

Finally, volume phase transitions of a liquid crystalline gel immersed in a nematogen [43, 44] are also closely related to the phase separations stated in this review.

References

[1] *Liquid Crystals in Complex Geometries*, edited by G. P. Crawford and S. Zumer (Taylor Francis, London, 1996).

[2] B. Kronberg, I. Bassignana, and D. Patterson, J. Phys. Chem. **82**, 1714 (1978).

[3] A. Dubaut, C. Casagrande, M. Veyssie, and B. Deloche, Phys. Rev. Lett. **45**, 1645 (1980).

[4] H. Orendi and M. Ballauff, Liq. Cryst. **6**, 497 (1989).

[5] W. Ahn, C. Y. Kim, H. Kim, and S. C. Kim, Macromolecules **25**, 5002 (1992).

[6] G. W. Smith, Phys. Rev. Lett. **70**, 198 (1993).

[7] F. Roussel, J. M. Buisine, U. Maschke, X. Coqueret, and F. Benmouna, Phys. Rev. E **62**, 2310 (2000).

[8] C. Shen and T. Kyu, J. Chem. Phys. **102**, 556 (1995).

[9] F. Brochard, J. Jouffroy, and P. Levinson, J. Phys. (France) **45**, 1125 (1984).

[10] M. Ballauff, Mol. Cryst. Liq. Cryst. **136**, 175 (1986).

[11] P. Maissa and P. Sixou, Liq. Cryst. **5**, 1861 (1989).

[12] R. Holyst and M. Schick, J. Chem. Phys. **96**, 721 (1992).

[13] T. Kyu and H. W. Chiu, Phys. Rev. E **53**, 3618 (1996).

[14] A. Matsuyama and T. Kato, J. Chem. Phys. **105**, 1654 (1996); Progr. Colloid Polym. Sci. **106**, 175 (1997).

[15] *Liquid Crystalline and Mesomorphic Polymers*, edited by V. P. Shibaev and L. Lam (Springer-Verlag, New York, 1993).

[16] P. J. Flory, Proc. R. Soc. London, Ser. A **234**, 60 (1956); **234**, 73 (1956).

[17] M. Warner and P. J. Flory, J. Chem. Phys. **73**, 6327 (1980).

[18] A. ten Bosch, P. Maissa, and P. Sixou, J. Chem. Phys. **79**, 3462 (1983).

[19] T. Sato and A. Teramoto, Adv. Polym. Sci. **126**, 85 (1996).

[20] A. Matsuyama, Y. Sumikawa, and T. Kato, J. Chem. Phys. **107**, 4711 (1997).

[21] A. Matsuyama and T. Kato, Phys. Rev. E **59**, 763 (1999); Phys. Rev. E **58**, 585 (1998); J. Chem. Phys. **109**, 2023 (1998).

[22] A. Matsuyama and T. Kato, J. Chem. Phys. **112**, 1046 (2000).

[23] P. J. Flory, *Principles of Polymer Chemistry* (Cornell University, Ithaca, 1953).

[24] W. Maier and A. Saupe, Z. Naturforsch, A **14a**, 882 (1959).

[25] P. G. de Gennes and J. Prost, *The Physics of Liquid Crystals*, 2nd ed. (Oxford. Sci., London, 1993).

[26] L. Onsager, Ann. N. Y. Acad. Sci. **51**, 626 (1949).

[27] A. Matsuyama and T. Kato, J. Chem. Phys. **108**, 2067 (1998).

[28] C. Casagrande, M. Veyssie, and C. M. Knobler, Phys. Rev. Lett. **58**, 2079 (1987).

[29] W. K. Kim and T. Kyu, Mol. Cryst. Liq. Cryst. **250**, 131 (1994).

[30] A. Nakai, T. Shiwaku, W. Wang, H. Hasegawa, and T. Hashimoto, Macromolecules **29**, 5990 (1996).

[31] A. Matsuyama, R. M. L. Evans, and M. E. Cates, Phys. Rev. E **61**, 2977 (2000); Mol. Cryst. Liq. Cryst. **367**, 455 (2001); A. Matsuyama and T. Kato, J. Chem. Phys. **113**, 9300 (2000).

[32] J. R. Dorgan and D. Yan, Macromolecules **31**, 193 (1998).

[33] A. J. Liu and G. H. Fredrickson, Macromolecules **29**, 8000 (1996).

[34] J. Fukuda, Phys. Rev. E **58**, R6939 (1998); **59**, 3275 (1999).

[35] H. W. Chiu and T. Kyu, J. Chem. Phys.**110**, 5998 (1999).

[36] A. M. Lapena, S. C. Glotzer, A. S. Langer, and A. J. Liu, Phys. Rev. E **60**, R29 (1999).

[37] *Solids far from equilibrium*, J. S. Langer, Chapter 13 (Cambridge University Press, New York, 1992).

[38] J. W. Cahn, Trans. Mat. Soc. AIME **242**, 166 (1968).

[39] S. P. Meeker, W. C. K. Poon, J. Crain, and E. M. Terentjev, Phys. Rev. E **61**, R6083 (2000).

[40] J. Yamamoto and H. Tanaka, Nature **409**, 321 (2001).

[41] M. Adams, Z. Dogic, S. L. Keller, and S. Fraden, Nature **393**, 349 (1998).

[42] A. Matsuyama and T. Kato, Eur. Phys. J. E **6**, 15 (2001).

[43] K. Urayama, Y. Okuno, T. Kawamura, and S. Kohjiya, Macromolecules **35**, 4567 (2002).

[44] A. Matsuyama and T. Kato, J. Chem. Phys. **114**, 3817 (2001); Phys. Rev. E **64**, 010701R (2001); J. Chem. Phys. **116**, 8175 (2002).